TÉCNICO LISBOA

Renewable Energy Sources and Dispersed Power Generation

Chapter 3

PV Power

Rui Castro

Edition 0 – September 2018

ABOUT THE AUTHOR

Rui Castro is a Professor at the Power Systems Section, Electrical and Computer Engineering Department of Técnico Lisboa (IST) and a researcher at INESC-ID/IST.

He lectures the IST Master's Courses on "Renewable Energy and Dispersed Power Generation" and "Economics and Energy Markets" and the PhD Course on "Renewable Energy Resources". He published two books, one on Renewable Energy and the other on Power Systems (in Portuguese). He has participated in several projects with the industry, namely with EDP group, REN (Portuguese Transmission System Operator) and ERSE (Portuguese Energy Regulator). In the last 3 years, he published more than 20 papers in top international journals, covering topics on renewable energy, impact of PV systems on the LV distribution grid, demand side management, offshore wind farms, energy resource scheduling on smart grids, water pumped storage systems, battery energy storage systems.

More details can be found at his website.

Readers are kindly asked to report any errors in this text to rcastro@tecnico.ulisboa.pt.

LIST OF ACRONYMS

AC – Alternating Current.

CSP – Concentrating Solar Power.

DC – Direct Current.

LCOE – Levelized Cost of Energy

MPPT – Maximum Power Point Tracker.

NOC – Normal Operating Conditions.

NOCT – Normal Operating Conditions Temperature.

PV – Photovoltaics.

RES – Renewable Energy Sources.

STC – Standard Test Conditions.

INDEX

1 INTRODUCTION

Portugal has valuable experience with regards to the integration of Renewable Energy Sources (RES) in the existing power system. The operating experience with the installation of large hydro plants was already significant when, in the period between the1980's and 1990's Portugal started deploying its first small hydro power plants. The installed capacity was relatively small due to several reasons including the difficulty of finding adequate locations. The main reason for the low amount of installed capacity can be attributed to the generous feed-in tariffs that were offered to the newly arriving wind power producers. This wind power phase started in the beginning of the 21st century and was characterized by the massive installation of wind turbine generators. This resulted in Portugal currently having a total installed capacity of 5 GW of wind power which is about one third of the total power generation capacity.

The integration of RES in the existing Portuguese power system has been successfully carried out with the necessity of RES curtailment being extremely rare. Nowadays, wind power accounts for about 25% of the Portuguese load supply.

Today, it is commonly accepted that the next stage of RES development will rely on Photovoltaic (PV) generators. This will take advantage of the impressive cost decrease that have been witnessed in recent years. Based on projects completed in 2017, the global weighted average Levelized Cost of Energy (LCOE) of large-scale solar PV plants is down 73% since 2010.

China added more solar PV capacity in 2017 than the world installed in 2015. The EU added about 6 GW of solar PV capacity in 2017, for a year-end total of nearly 108 GW. Asia eclipsed all other regions, accounting for 75% of global additions. The current installed PV capacity in Portugal is still modest (about 0.5 GW at the end of 2017), but the expectation is that it will steadily increase in the coming years.

As anticipated by the introduction, the present text will approach solely the high power applications of PV power, the so-called utility scale PV parks. Medium power applications, used in rural electrification and microgeneration installed near the end-users, and low power applications, used in watches and pocket calculators, battery chargers, road signals, parking meters, etc., are out of the scope of this text.

2 BASIC CONCEPTS

2.1 SOME DEFINITIONS

The study of PV power requires some prior definitions to provide the context. Here they are:

- Irradiance – The solar power; it is represented by *G* and is measured in W/m^2.
- Irradiation (Insolation) – The solar energy; it is represented by H_i and is measured in Wh/m^2.
- Peak Power – The peak-power; it is represented by P_p and is measured in W_p. It is the PV module electrical output DC power under Standard Test Conditions (STC).
- Standard Test Conditions – The internationally agreed conditions by the manufacturers to perform the PV modules factory tests. They are defined as $G^r = 1000 \ \text{W/m}^2$ and module temperature $\theta_m^r = 25 \ ^\circ\text{C} \Leftrightarrow T^r = 298 \ \text{K}$. In the sequence, the quantities referenced by the superscript *r* are considered to refer to STC.

2.2 PERFORMANCE INDEXES

The efficiency at STC is defined as (*A* is the module area):

$$\eta^r = \frac{P_p}{G^r A} \qquad \text{equation 2.1}$$

The efficiency at other irradiance (*G*) and module temperature (*T*) conditions is:

$$\eta = \frac{P_{DC}(G,T)}{GA} \qquad \text{equation 2.2}$$

where $P_{DC}(G,T)$ is the PV module DC output power for the given irradiance and temperature conditions.

The utilization of peak power is:

$$h_a = Y_F = \frac{E_a}{P_p}$$

equation 2.3

where E_a is the annual electricity yield injected in the grid by the PV module. In Portugal, this index changes between 1500 h (in the northern part) to around 1800 h (in the southern part).

The reference index is:

$$Y_r = \frac{H_i}{G^r}$$

equation 2.4

The performance ratio is defined as:

$$PR = \frac{Y_F}{Y_r} = \frac{E_a}{\eta^r A H_i}$$

equation 2.5

that is, the ratio between the electricity injected in the grid and the one that would have been produced by the PV module if the efficiency was constant and equal to the efficiency at STC. Typical values for PR lay between 0.7 and 0.8.

2.3 PV System Equipment

A typical PV system is comprised of the equipment showed in Figure 2-1.

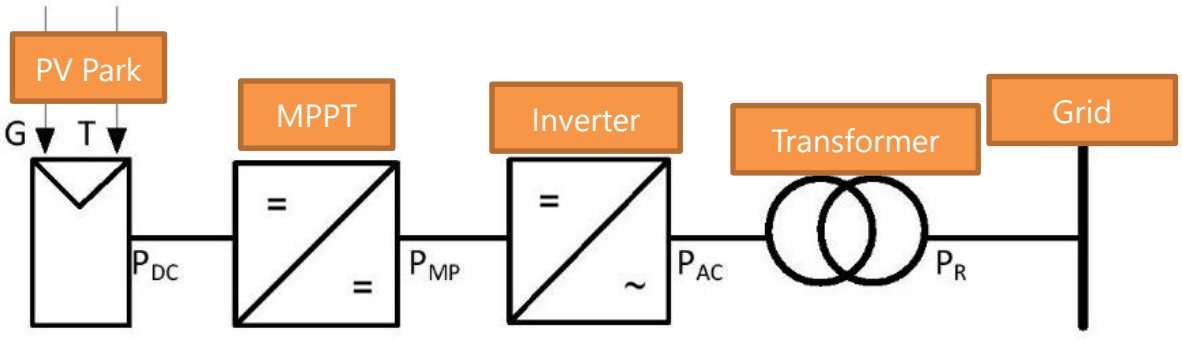

Figure 2-1: PV system equipment.

The MPPT is a Maximum Power Point Tracker that optimizes the operating point of the PV module and extracts the maximum possible power from it, given the

conditions of irradiance and temperature. The inverter is a DC/AC converter, which is required because the operating principle of PV modules implies DC (Direct Current) power is produced. However, the power system operates in AC (Alternating Current), thus an inverter is needed. Both devices are described further on this text.

The transformer is a device that transforms the AC output voltage to the adequate level to be injected in the grid. Details about DC, AC and transformers can be found in the companion text, "AC Electric Circuits for Non-Electrical Engineers".

To increase their utility (the output voltage of a single PV cell is typically 0.5 V), a number of individual PV cells are interconnected together in a sealed, weather-proof package called a Module. For example, it is common to have modules composed of 72 PV cells connected in series. The characteristic parameters of PV modules are given in the datasheets. To achieve the desired voltage and current, modules are wired in series and parallel into what is called a PV Array. The flexibility of the modular PV system allows designers to create solar power systems that can meet a wide variety of electrical needs. Figure 2-2 shows a PV cell, a module and an array.

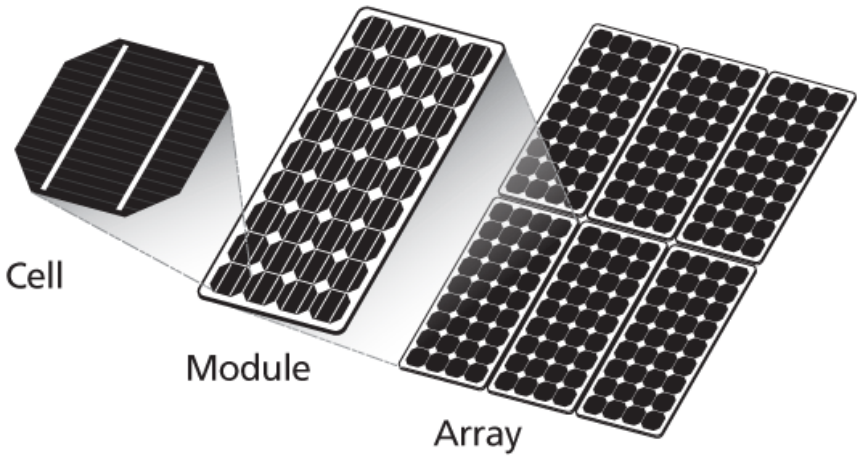

Figure 2-2: PV cells, modules and arrays; Source: http://www.samlexsolar.com/learning-center/solar-cell-module-array.aspx

A number of PV arrays connected in series and parallel, together with the inverters and transformer, compose a PV park, as shown in Figure 2-3.

Figure 2-3: PV park in Portugal.

2.4 PV CELL OPERATING PRINCIPLE

All other generation technologies, as for instance, hydro, coal, combined cycle, wind, use the same operating principle based on a turbine coupled with a generator. PV technology shows a completely different approach.

First of all, we require a material with the appropriate characteristics. Silicon is the most used material for PV conversion. Silicon has 14 electrons, with 4 electrons in the valence band. To achieve the desired objective of having 8 electrons in the valence band, each atom of silicon makes 4 bonds with 4 neighbour atoms, sharing one electron with each one of the neighbours, as seen in Figure 2-4. These bonds are called covalent bonds. In this way, the valence band is full and we have a stable connection.

The particles that compose the sun radiation are the photons. When the silicon crystal is exposed to sun light, photons with enough energy, higher than the silicon energy gap band, 1.12 eV, can displace electrons to the conduction band and originate hole–electron pairs.

If nothing else was done, the free electrons would return to the valence band after a while, because no electric field would keep them in the conduction band.

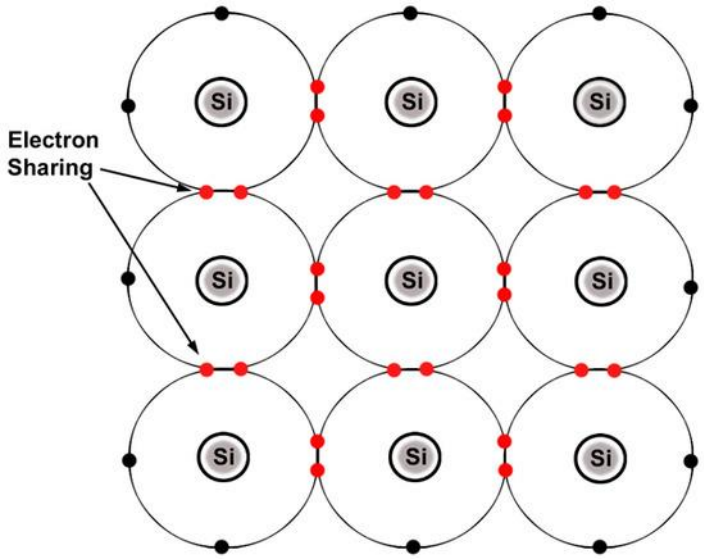

Figure 2-4: Silicon covalent bonds; Source: https://photon.libretexts.org/The_Science_of_Solar/Solar_Basics/A._Introductory_Physics_for_Solar_Application/I._Atoms_and_Materials/4._Covalent_Bonds.

So, we need to create an electric field to keep the free electrons in the conduction band. This is achieved by doping the silicon. The doping process consists in injecting, in one side of the crystal, a material with one less electron than silicon, for instance boron. This way, a positive zone has been created, the silicon type *p* zone. On the other side, we inject a material with one more electron, for instance, phosphorus, therefore, creating a negative zone, the silicon type *n* zone.

In this way, we created an electrical field, the so-called *p-n* junction. In the presence of this electric field, holes will be accelerated to the + terminal; electrons will be accelerated to the – terminal, and a DC current is produced.

A diagram of this process can be seen in Figure 2-5.

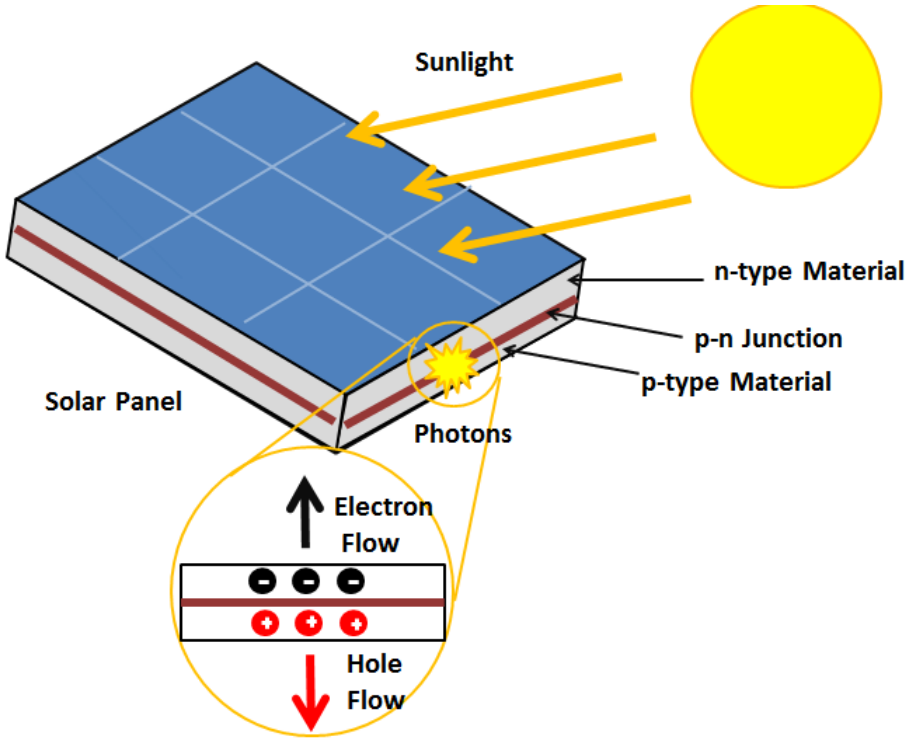

Figure 2-5: PV effect; Source: https://energyeducation.ca/encyclopedia/Photovoltaic_effect.

2.5 A Note on PV Costs

It is well known that PV costs experienced an amazing cost reduction in the past years. Just to have an idea about the magnitude of the cost reduction, Figure 2-6 is offered.

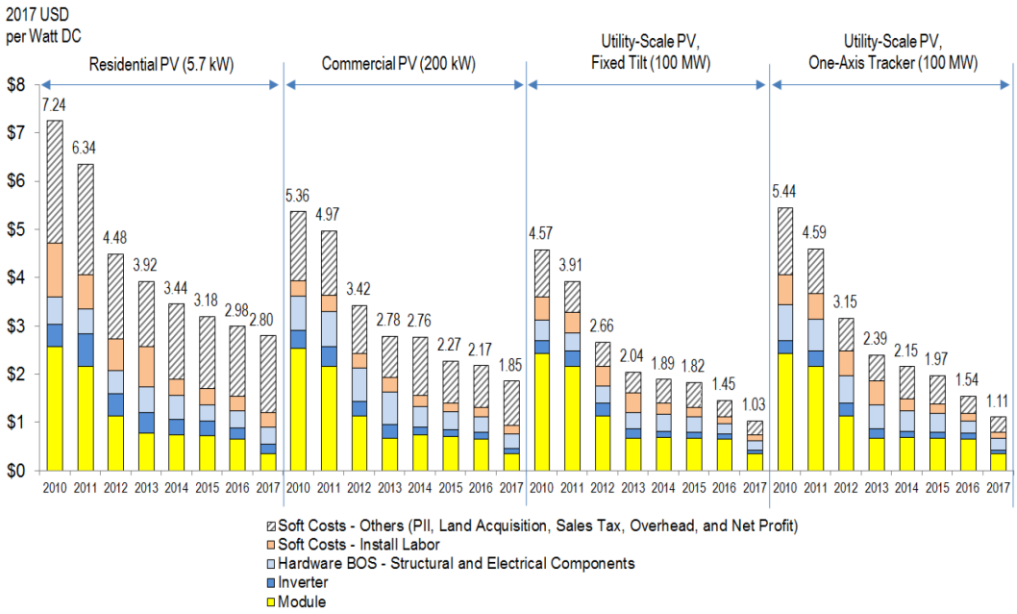

Figure 2-6: PV cost reduction; Source: NREL, USA, 2017.

This figure shows an impressive cost reduction over the past years for all PV segments: Residential, Commercial, Utility-Scale Fixed Tilt and Utility-Scale One-Axis Tracker. For instance, currently PV electricity production cost is around 1USD/Wp for utility-scale and around 3USD/Wp for households. These figures are in line with European ones.

3 PV PERFORMANCE MODELS

In this chapter, the theoretical backgrounds of commonly used PV performance model are presented. These models are simplified FE (Fast Estimate) and the intermediate 1D + 3P (1 Diode + 3 Parameters).

3.1 DATA PROVIDED BY MANUFACTURERS IN DATASHEETS

Manufacturers of PV modules provide datasheets detailing the characteristics of their products. Table 3-1 shows the data commonly provided by the manufacturers.

Table 3-1: Data commonly provided by manufacturers in PV modules datasheets.

Symbol	Unit	Description
$P_{MP}^{r} = P_{p}$	Wp	Peak power – Maximum DC power output @STC.
V_{MP}^{r}	V	Output voltage at maximum power @STC.
I_{MP}^{r}	A	Output current at maximum power @STC.
V_{oc}^{r}	V	Open circuit voltage @STC.
I_{sc}^{r}	A	Short-circuit current @STC.
NOCT	ºC	Normal Operating Conditions Temperature (NOCT) – Module temperature in Normal Operating Conditions (NOC) defined as: irradiance = 800 W/m^2 and ambient temperature = 20ºC.
μ_{Isc}	%/ºC	Temperature coefficient of the short-circuit current.
μ_{Voc}	%/ºC	Temperature coefficient of open circuit voltage.
μ_{Pp}	%/ºC	Peak power temperature coefficient.
N_s		Number of cells connected in series in the module.
P_{MP}^{NOC}	W	Maximum DC power output under NOC.
V_{MP}^{NOC}	V	Voltage at maximum power under NOC.

I_{MP}^{NOC}	A	Current at maximum power under NOC.
V_{oc}^{NOC}	V	Open-circuit voltage under NOC.
I_{sc}^{NOC}	A	Short-circuit current under NOC.

3.2 SIMPLIFIED MODEL – FAST ESTIMATE (FE)

To establish a simple model to describe the behaviour of a PV module, it is assumed that the DC power output depends linearly on the irradiance, *G*, and the temperature correction is included through the peak power temperature coefficient, μ_{Pp}, usually supplied in the manufacturer's datasheets.

$$P(G,T) = \frac{G}{G^r} P_p \left[1 + \mu_{Pp}\left(T - T^r\right)\right]$$

equation 3.1

The advantage of this model is its simplicity; the disadvantage is that it does not allow the access to other quantities of interest, such as the maximum power voltage, the maximum power current, the open-circuit voltage or the short-circuit current.

3.3 INTERMEDIATE MODEL – 1 DIODE AND 3 PARAMETERS (1D+3P)

We highlight that we are seeking for a model that is able to compute the PV module DC output power for any given irradiance and temperature conditions.

With this objective in mind, a more sophisticated model can be constructed by assuming that the PV module can be described by the equivalent electric circuit shown in Figure 3-1.

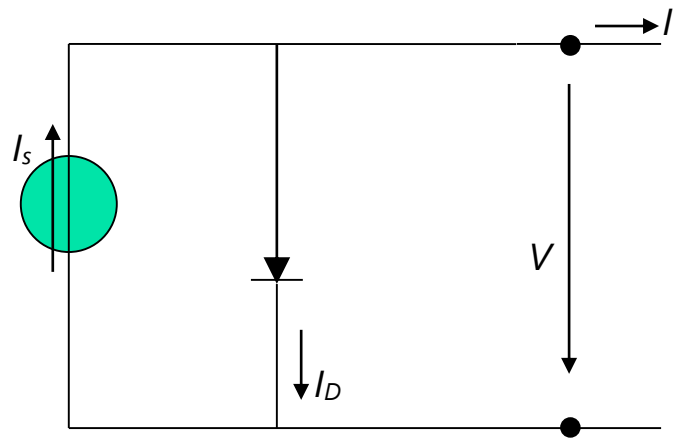

Figure 3-1: Equivalent circuit of a PV module – 1D+3P model.

The *pn* junction acts like a large diode. The fundamental property of a diode is that it conducts electric current in only one direction. When the applied voltage is positive and greater than a certain minimum, then current flows through the diode. If the voltage is negative, then the diode does not conduct current, at least until a certain voltage is reached. Figure 3-2 helps in understanding the process.

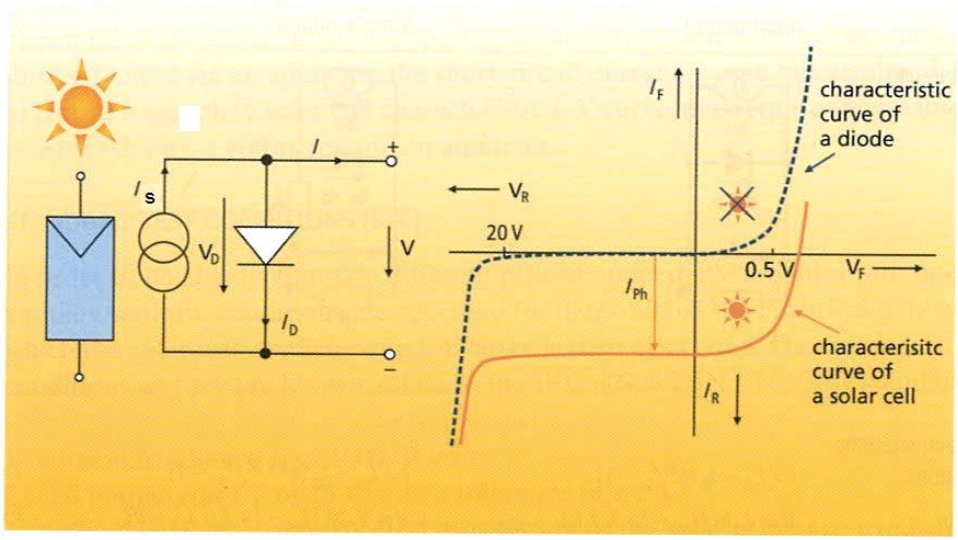

Figure 3-2: Sun power source + diode.

Current I_D is the current across a diode, whose equation is given by equation 3.2 and the graphics is displayed in Figure 3-2.

$$I_D = I_0\left(e^{\frac{V}{mV_T}} - 1\right) \qquad \text{equation 3.2}$$

where: I_0 – Diode's inverse saturation current; V – Terminal voltage; m – Diode's ideality factor (ideal diode: $m = 1\times N_s$; real diode: $m > 1\times N_s$);

Still regarding equation 3.2, V_T is the thermal voltage in V, given by:

$$V_T(T) = \frac{K}{q}T \qquad \text{equation 3.3}$$

where: K is the Boltzmann constant (K=1.38×10^{-23} J/K), T is the absolute temperature in K and q is the electron's electrical charge (q = 1.6×10^{-19} C). For the STC temperature, it is $V_T^r = 0.0257$ V.

Current I_S is represented by a current source and is the current generated by the beam of light radiation photons, upon reaching the active surface of the module (photovoltaic effect); this unidirectional current is constant for a given incident irradiance. As mentioned, the *p-n* junction operates as a diode crossed by a unidirectional internal current I_D, which depends on the terminal voltage V.

Referring to Figure 3-1, current I is:

$$I = I_s - I_D = I_s - I_0\left(e^{\frac{V}{mV_T}} - 1\right) \qquad \text{equation 3.4}$$

Our first task will be to find out if the electric circuit represented in Figure 3-1 is able to describe the behaviour of a PV cell with an appropriate degree of accuracy.

With this objective in mind, we note that the source current, I_S, is equal to the short-circuit current, I_{sc}, as can be seen from equation 3.4, by setting V=0. In the same equation, if we set I=0, we can derive an equation for the inverse saturation current, as:

$$I_0 = \frac{I_{sc}}{e^{\frac{V_{oc}}{m\,V_T}} - 1} \qquad \text{equation 3.5}$$

Replacing equation 3.5 in equation 3.4 and taking into consideration that $e^{\frac{V_{oc}}{mV_T}} >> 1$; $e^{\frac{V}{mV_T}} >> 1$, we obtain:

$$I = I_{sc}\left(1 - e^{\frac{V - V_{oc}}{mV_T}}\right) \qquad \text{equation 3.6}$$

For a given PV cell with and area of 0.01 m^2, we have measured the following values: G = 430 W/m^2; T = 25ºC, I_{sc} = 1.28 A; V_{oc} = 0.56 V. Then, we applied different voltage values and measured the corresponding current. The experimental I-V graphic is shown in Figure 3-3 by the blue dots.

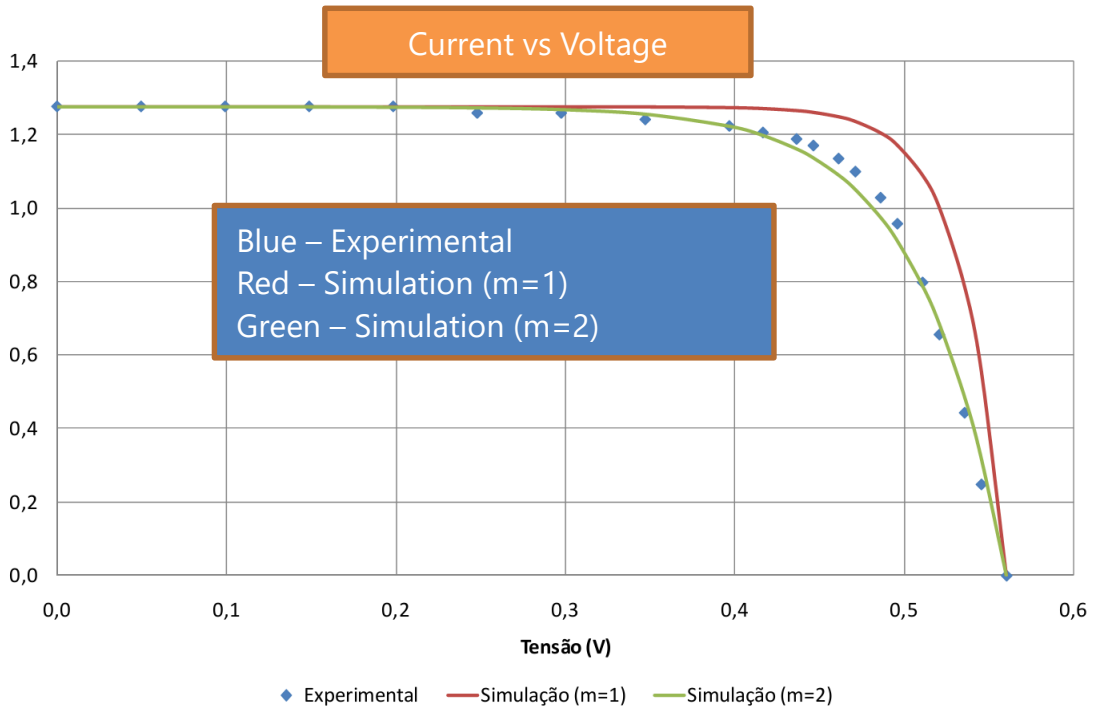

Figure 3-3: 1D+3P model validation against experimental results.

Then we proceeded to the simulation. By replacing T, I_{sc} and V_{oc} in equation 3.6, we can give values to V and compute the corresponding I. We note that m is still unknown, and till now we have not found out a way to compute it. As so, let us for the time being impose m=1, which represents an ideal diode in the circuit of Figure 3-1.

The obtained results are shown in Figure 3-3 by the red solid line. We were unable to reproduce the experimental results, even when we tried m=2, as shown by the green line in Figure 3-3. Nevertheless, the shape of the curves is fairly similar, which

indicates that there exists a *m* value, which allows for the experimental curve to be reproduced through simulation. This validates our 1D+3P model.

Let us go on with the computation of the DC power. For a given irradiance and module temperature, the electrical DC output power, *P*, is:

$$P = VI = V\left[I_{sc} - I_0\left(e^{\frac{V}{mV_T}} - 1 \right) \right]$$

equation 3.7

The maximum power is obtained when $dP/dV = 0$, which leads to:

$$I_{sc} + I_0\left(1 - e^{\frac{V}{mV_T}} - \frac{V}{mV_T} e^{\frac{V}{mV_T}} \right) = 0$$

$$e^{\frac{V}{mV_T}} = \frac{\frac{I_{sc}}{I_0} + 1}{\frac{V}{mV_T} + 1}$$

equation 3.8

The determination of the maximum power is of utmost importance, because PV modules are equipped with a power electronic device, the Maximum Power Point Tracker (MPPT), which ensures the module operates at maximum power given the existent irradiance and temperature conditions. As so, we keep our objective in mind, which is to be able to compute the maximum PV module DC output power, given the module temperature and irradiance.

The solution to equation 3.8 is $V = V_{MP}$, the maximum power voltage, and the corresponding current is $I = I_{MP}$, the maximum power current, respectively given by:

$$V_{MP} = mV_T \ln\left(\frac{\frac{I_{sc}}{I_0} + 1}{\frac{V_{MP}}{mV_T} + 1} \right)$$

equation 3.9

$$I_{MP} = I_{sc} - I_0\left(e^{\frac{V_{MP}}{mV_T}} - 1 \right)$$

equation 3.10

The maximum power, hereafter denoted by P_{DC} to highlight it is DC power, is $P_{MP} = V_{MP} I_{MP} = P_{DC}$.

As equation 3.9 is a non-linear equation, its solution requires iterative methods. If Gauss-Seidel is used, the required iterative equation to be solved is (*k* is the iteration number):

$$V_{MP}^{(k+1)} = mV_T \ln\left(\frac{\frac{I_{sc}}{I_0}+1}{\frac{V_{MP}^{(k)}}{mV_T}+1}\right) \qquad \text{equation 3.11}$$

To solve equation 3.11, we need a starting guess, $V_{MP}^{(0)}$, and the knowledge of the three parameters *m*, I_0 and I_{sc}. We recall that the thermal voltage is known, because it depends solely on the module temperature, which we assume it is known.

A proper starting guess is $V_{MP}^{(0)} = V_{MP}^{r}$. We will now proceed with the determination of the three parameters of the model at STC.

First of all, let us write the fundamental equation 3.4 at the short-circuit ($V = 0$) open-circuit ($I = 0$), and maximum power ($V = V_{MP}$; $I = I_{MP}$) points, respectively, and at STC:

$$I_{sc}^{r} = I_{s}^{r} \qquad \text{equation 3.12}$$

$$0 = I_{sc}^{r} - I_0^{r}\left(e^{\frac{V_{oc}^{r}}{m^{r}V_T^{r}}} - 1\right) \qquad \text{equation 3.13}$$

$$I_{MP}^{r} = I_{sc}^{r} - I_0^{r}\left(e^{\frac{V_{oc}^{r}}{m^{r}V_T^{r}}} - 1\right) \qquad \text{equation 3.14}$$

We immediately conclude that equation 3.12 portrays the first equation we are looking for. The parameter I_{sc}^{r} is directly given in the module datasheet, as seen in Table 3-1.

From equation 3.13, we obtain the second parameter:

$$I_0^r = \frac{I_{sc}^r}{e^{\frac{V_{oc}^r}{m^r V_T^r}} - 1}$$

equation 3.15

where V_{oc}^r is the open-circuit voltage at STC.

Finally, the third parameter is obtained by replacing equation 3.15 into equation 3.14, thereby leading to:

$$m^r = \frac{V_{MP}^r - V_{oc}^r}{V_T^r \ln\left(1 - \frac{I_{MP}^r}{I_{sc}^r}\right)}$$

equation 3.16

It is important to highlight that the 3 parameters of the model can be computed solely based on datasheet open information, as can be verified in Table 3-1.

Now, the conditions are met to compute the maximum power voltage, given by equation 3.11, at STC, the obtained result being:

$$V_{MP}^{r\ (k+1)} = m^r V_T^r \ln\left(\frac{\frac{I_{sc}^r}{I_0^r} + 1}{\frac{V_{MP}^{r\ (k)}}{m^r V_T^r} + 1}\right)$$

equation 3.17

Of course, this has absolutely no interest at all, because the STC maximum power voltage is given at the module datasheet, and therefore is known. What would be interesting is to find the maximum power voltage for irradiance and temperature conditions different from STC.

Before that, it would be interesting to see how an I-V and a P-V curve look like for STC. The relevant equations are equation 3.4 and equation 3.7 that we recover here written for STC.

$$I = I_{sc}^r - I_0^r\left(e^{\frac{V}{m^r V_T^r}} - 1\right)$$

equation 3.18

$$P = VI$$

equation 3.19

Based on datasheet information, we can compute the 3 parameters of the 1D+3P model and give values to *V* and compute the corresponding *I*. The obtained result is shown in Figure 3-4.

One can observe the peak-power, i.e., the I-V point of maximum power under STC. The peak power, P_p, is defined as the PV cell DC output power at STC (G^r=1000 W/m^2 and T^r=298 K (25ºC)). In fact, we have:

$$P_p = V_{MP}^r I_{MP}^r = P_{DC}^r \qquad \text{equation 3.20}$$

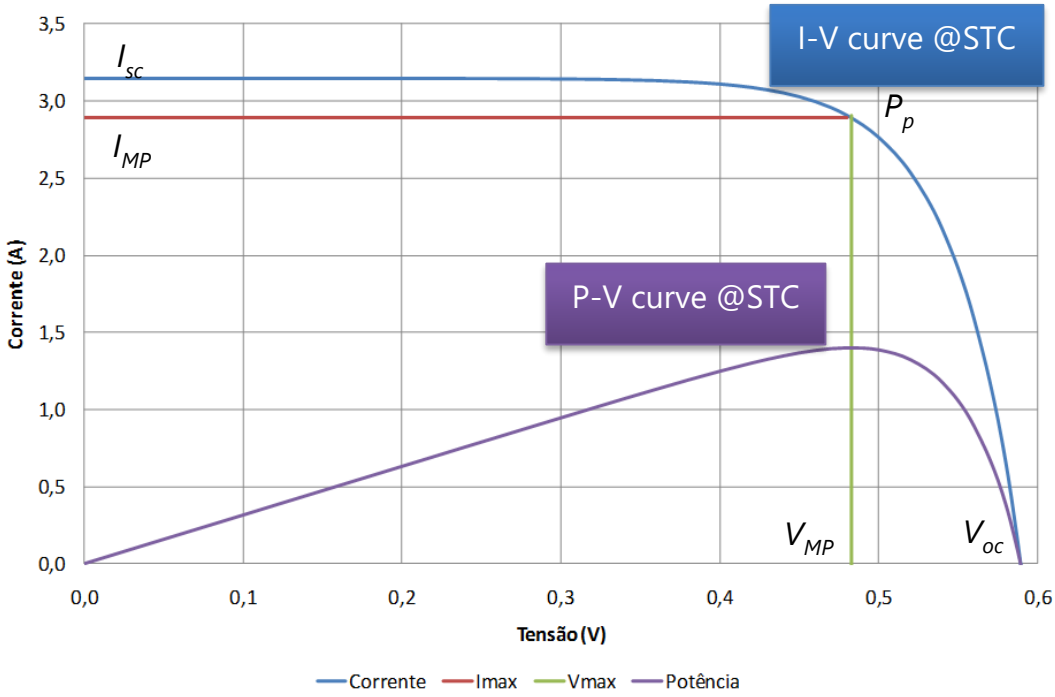

Figure 3-4: I-V and P-V curves @STC.

One quantity that is usually defined to account for the performance of a PV module is the Fill Factor at STC, defined as:

$$FF^r = \frac{P_p}{V_{oc}^r I_{sc}^r} \qquad \text{equation 3.21}$$

The maximum voltage of a PV module is V_{oc}^r and the maximum current is I_{sc}^r. However, at both of these operating points, the power from the PV module is zero. So, the product $V_{oc}^r I_{sc}^r$ is impossible to attain. The fill factor is defined as the ratio between two areas, as shown in Figure 3-5.

The fill factor is always less than one, the higher the fill factor the best. Typical FF of a PV silicon module is between 0.7 and 0.8.

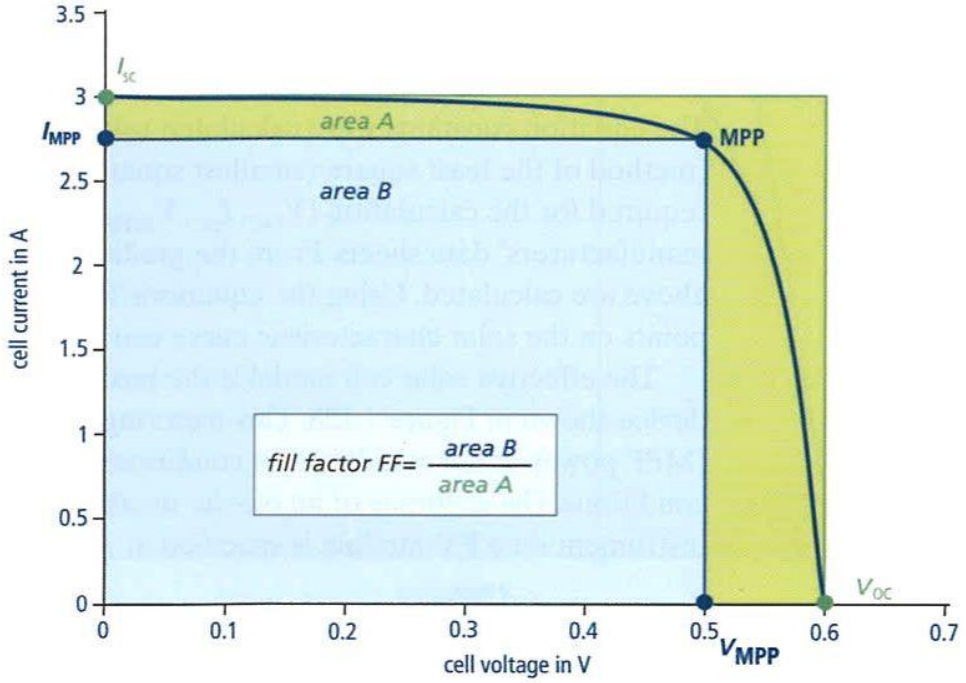

Figure 3-5: Fill Factor of a PV cell.

Influence of irradiance and temperature

The influence of the irradiance and module temperature in the 1 diode and 3 parameters model is included by making the following approximations:

- the ideality factor is constant $m^r = m$;
- the module temperature influence is accounted for in the inverse saturation current, $I_0 = I_0(T)$;
- the variation of the irradiance is incorporated in the short-circuit current, $I_{sc} = I_{sc}(G)$.

These approximations are justified by experimental evidence.

Therefore, for any temperature and irradiance given conditions, equation 3.11 can be written as:

$$V_{MP}^{(k+1)}(G,T) = mV_T(T)\ln\left(\frac{\frac{I_{sc}(G)}{I_0(T)}+1}{\frac{V_{MP}^{(k)}}{mV_T(T)}+1}\right) \qquad \text{equation 3.22}$$

It remains to be explained how are we going to incorporate the influence of the temperature on the inverse saturation current and the influence of the irradiance on the short-circuit current.

Let us begin by the former. It falls outside the scope of this course, but it is possible to demonstrate that the simplest model accounts for the inverse saturation current dependence on the temperature by:

$$I_0(T) = DT^3 e^{\frac{-N_s\varepsilon}{mV_T(T)}} \qquad \text{equation 3.23}$$

where *D* is a constant, ε=1.12 eV is the silicon bandgap and Ns is the number of series connected cells in a PV module. The value of D is not relevant, because we can write equation 3.23 at STC as:

$$I_0^r = DT^{r3} e^{\frac{-N_s\varepsilon}{mV_T^r}} \qquad \text{equation 3.24}$$

Dividing equation 3.23 by equation 3.24, we obtain the relationship we are looking for:

$$I_0(T) = I_0^r\left(\frac{T}{T^r}\right)^3 e^{\frac{N_s\varepsilon}{m}\left(\frac{1}{V_T^r}-\frac{1}{V_T(T)}\right)} \qquad \text{equation 3.25}$$

We can plot the I-V curve for different temperatures, keeping the irradiance at its STC value (G^r=1000 W/m^2). This is achieved by using fundamental equation 3.4, written at the appropriate operating point, as follows:

$$I = I_{sc}^r - I_0(T)\left(e^{\frac{V}{mV_T(T)}}-1\right) \qquad \text{equation 3.26}$$

The obtained result is depicted in Figure 3-6.

We can conclude that the output power drops as the temperature increases, which is a known drawback of PV modules.

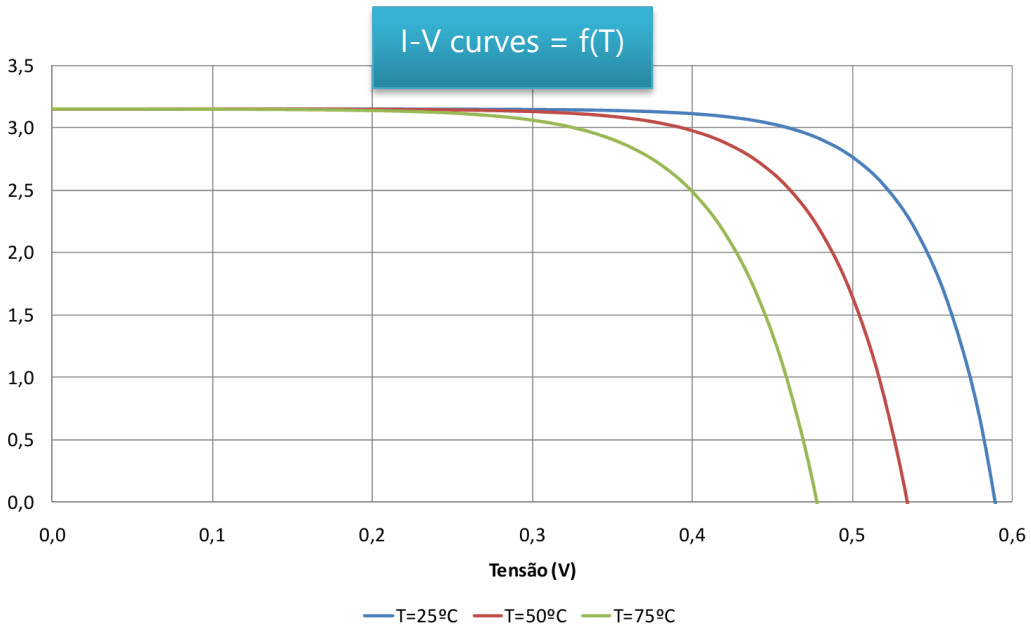

Figure 3-6: I-V curves for different temperatures; $G = G^r$.

As for the influence of the irradiance on the short-circuit current, we are going to use the simplest model, that states that the short-circuit current is linearly dependent on the irradiance:

$$I_{sc}(G) = I_{sc}^r \frac{G}{G^r} \qquad \text{equation 3.27}$$

We highlight that the irradiance influences the inverse saturation current and the temperature influence the short-circuit current, but we are neglecting these variations, as experimental evidence shows that they are minor.

In a similar way that we have done for the temperature, we can compute the I-V curves for different irradiances, keeping the temperature at its STC value (T^r = 298 K), as shown in Figure 3-7.

The used equation is now as follows:

$$I = I_{sc}(G) - I_0^r \left(e^{\frac{V}{mV_T^r}} - 1 \right) \qquad \text{equation 3.28}$$

It is concluded that the output power increases with the irradiance, as it would be expected. Higher solar power would give rise to more PV output power.

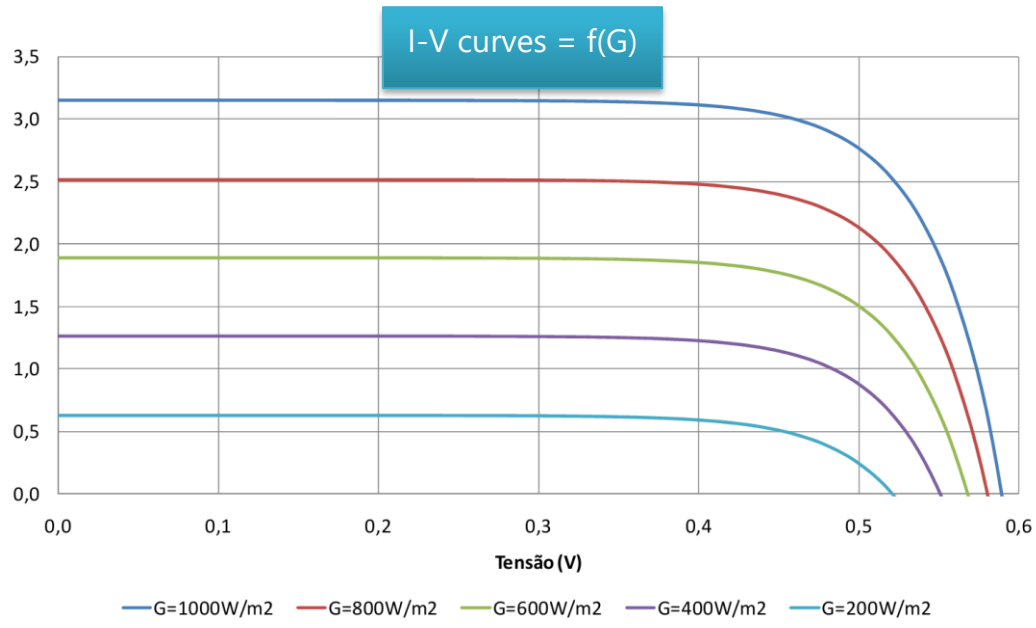

Figure 3-7: I-V curves for different irradiances; T = T^r.

We are now able to compute the maximum power voltage for any irradiance and temperature conditions, iteratively solving equation 3.22, taking into account equation 3.16, equation 3.3, equation 3.27 and equation 3.25. After V_{MP} (G,T) is obtained, the maximum power current is computed through (see equation 3.10, which is derived from the fundamental equation 3.4):

$$I_{MP}(G,T) = I_{sc}(G) - I_0(T)\left(e^{\frac{V_{MP}(G,T)}{mV_T(T)}} - 1 \right) \qquad \text{equation 3.29}$$

The DC power output is finally computed by multiplying equation 3.22 by equation 3.29.

Simplified computation process of *PDC*

Let us look again at equation 3.29. We notice that it can be written as follows:

$$V_{MP}(G,T) = mV_T(T)\ln\left(\frac{I_{sc}(G) - I_{MP}(G,T)}{I_0(T)} \right) \qquad \text{equation 3.30}$$

The issue in this equation is that I_{MP} depends on V_{MP}. If the aim is to simplify the computation process, we can introduce a simplification to overcome this problem. As so, let us assume the maximum power current changes linearly with the irradiance, as we have assumed for the short-circuit current:

$$I_{MP}(G) = I_{MP}^{r} \frac{G}{G^{r}}$$

equation 3.31

Experimental evidence shows that considering the short-circuit current changing linearly with the irradiance is a fairly good approximation. For the maximum power current, the approximation is not so good, but we are going to use it for the sake of simplification.

This considerably simplifies the computation process, as now V_{MP} can be easily calculated, without the need of iterations.

$$V_{MP} = mV_T \ln\left(\frac{\frac{G}{G^{r}}(I_{sc} - I_{MP})}{I_0^{r}\left(\frac{T}{T^{r}}\right)^{3} e^{\frac{N_s \varepsilon}{m}\left(\frac{1}{V_T^{r}} - \frac{1}{V_T}\right)}}\right)$$

equation 3.32

The DC power output is obtained from the multiplication of algebraic equation 3.31 and equation 3.32.

Example 3—1:

The datasheet of a PV module is known and given in the table below.

For the Normal Operating Conditions, the datasheet indicates P_{DC}=72.3 W.

Compute the output power for NOC and the respective error using:

- *The 1D+3P model*
- *The 1D+3P model with the simplified computation (SC) of PDC*
- *The fast estimate (FE)*

Monocrystalline Silicon			
Peak power	P_p	*100.3*	Wp
Maximum power current	I_{MP}^r	*5.9*	A
Maximum power voltage	V_{MP}^r	*17.0*	V
Short-circuit current	I_{sc}^r	*6.5*	A
Open-circuit voltage	V_{oc}^r	*21.0*	V
NOCT	*NOCT*	*45*	ºC
Temperature coefficient Pp	μ_{Pp}	*–0.45*	%/ºC
Temperature coefficient Icc	μ_{Isc}	$2.80x10^{-3}$	A/ºC
Temperature coefficient Vca	μ_{Voc}	$–7.60x10^{-2}$	V/ºC
Number of cells in series	*Ns*	*36*	
Length	*C*	*1.316*	m
Width	*L*	*0.660*	m

First of all, let us recall that the NOC are G^{NOC} = 800 W/m^2 and T^{NOC} = 318 K.

The 3 parameters of the model are computed for STC and are given by (:

$$m^r = \frac{V_{MP}^r - V_{oc}^r}{V_T^r \ln\left(1 - \frac{I_{MP}^r}{I_{sc}^r}\right)} = 65.38$$

$$I_0^r = \frac{I_{sc}^r}{e^{\frac{V_{oc}^r}{m^r V_T^r}} - 1} = 2.40 \times 10^{-5} \text{ A}$$

$$I_{sc}^{r} = 6.50 \text{ A}$$

The influence of irradiance and temperature is accounted for in the short-circuit current and inverse saturation current, respectively:

$$I_{sc}(G^{NOC}) = I_{sc}^{r}\frac{G^{NOC}}{G^{r}} = 5.2 \text{ A}$$

$$I_0(T^{NOC}) = I_0^{r}\left(\frac{T^{NOC}}{T^{r}}\right)^3 e^{\frac{N_s\varepsilon}{m}\left(\frac{1}{V_T^{r}}-\frac{1}{V_T(T^{NOC})}\right)} = 1.32\times10^{-4} \text{ A}$$

Also, the thermal voltage depends on the temperature:

$$V_T(T^{NOC}) = \frac{K}{q}T^{NOC} = 0.0274 \text{ V}$$

1.

First we have to compute the maximum power voltage at NOC using the Gauss-Seidel iterative process:

$$V_{MP}^{(k+1)}(G^{NOC},T^{NOC}) = mV_T(T^{NOC})\ln\left(\frac{\frac{I_{sc}(G^{NOC})}{I_0(T^{NOC})}+1}{\frac{V_{MP}^{(k)}}{mV_T(T^{NOC})}+1}\right)$$

Here are the steps of the iterative procedure:

$$V_{MP}^{(0)} = V_{MP}^{r} = 17 \text{ V}$$
$$V_{MP}^{(1)} = 14.74 \text{ V}$$
$$V_{MP}^{(2)} = 14.97 \text{ V}$$
$$V_{MP}^{(3)} = 14.95 \text{ V}$$
$$V_{MP}^{(4)} = 14.95 \text{ V}$$

We stop the iterative process when the difference between V_{MP} computed in two consecutive iterations is lower than a pre-defined tolerance ε (typically $\varepsilon=10^{-2}$).

$$\left|V_{MP}^{(k)} - V_{MP}^{(k-1)}\right| < \varepsilon$$

After the 4th iteration the final result is obtained:

$$V_{MP}^{(4)} = 14.95 \text{ V} = V_{MP}(G^{NOC}, T^{NOC})$$

Now, we can compute the maximum power current as:

$$I_{MP}(G^{NOC}, T^{NOC}) = I_{sc}(G^{NOC}) - I_0(T^{NOC})\left(e^{\frac{V_{MP}(G^{NOC}, T^{NOC})}{mV_T(T^{NOC})}} - 1 \right) = 4.64 \text{ A}$$

and the DC output power is:

$$P_{DC}(G^{NOC}, T^{NOC}) = V_{MP}(G^{NOC}, T^{NOC}) I_{MP}(G^{NOC}, T^{NOC}) = 69.43 \text{ W}$$

The error relative to the datasheet value is:

$$\text{error} = \frac{P_{DC}(G^{NOC}, T^{NOC}) - P_{DC}}{P_{DC}} = -3.97\%$$

2.

Using the simplified computation (SC) of PDC, we assume that:

$$I_{MP}(G^{NOC}) = I_{MP}^{r} \frac{G^{NOC}}{G^{r}} = 4.72 \text{ A}$$

The maximum power voltage can therefore be computed as:

$$V_{MP}(G^{NOC}, T^{NOC}) = mV_T(T^{NOC}) \ln\left(\frac{I_{sc}(G^{NOC}) - I_{MP}(G^{NOC})}{I_0(T^{NOC})} \right) = 14.69 \text{ V}$$

The final result achieved by this SC process is:

$$P_{DC}(G^{NOC}, T^{NOC}) = V_{MP}(G^{NOC}, T^{NOC}) I_{MP}(G^{NOC}) = 69.32 \text{ W}$$
$$\text{error} = -4.12\%$$

3.

If the FE method is used, the final result is:

$$P(G^{NOC}, T^{NOC}) = \frac{G^{NOC}}{G^{r}} P_p \left[1 + \mu_{Pp} \left(T^{NOC} - T^{r} \right) \right] = 73.02 \text{ W}$$
$$\text{error} = 0.99\%$$

Surprisingly, the FE method achieved the best estimation. FE method usually performs well, the problem being that it does not provide any information about other relevant quantities, such as, voltages and currents.

3.4 Grounds of the Detailed model – 1 diode and 5 parameters (1D+5P)

The equivalent circuit of this model is represented in Figure 3-8. It accounts for several losses that exist in a PV module.

Once again, the initial objective is to be able to compute the 5 model parameters – I_s^r, I_0^r, m, R_s e R_{sh} – which are based solely on the manufacturer's datasheet, namely: V_{oc}^r, I_{sc}^r, V_{MP}^r, I_{MP}^r, μ_{Isc} and μ_{Voc}. Then, the final objective would be to compute the DC output power for any given irradiance and temperature conditions.

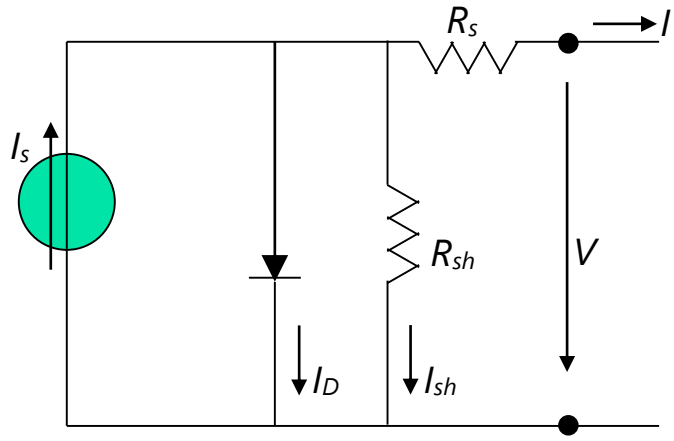

Figure 3-8: Equivalent circuit of a PV module – 1D+5P model.

In this case, current I can be written as:

$$I = I_s - I_D - I_{sh} = I_s - I_0\left(e^{\frac{V+R_sI}{mV_T}} - 1\right) - \frac{V+R_sI}{R_{sh}}$$

equation 3.33

The development of the 1D+5P model is outside the scope of this introductory course.

4 PV SYSTEM COMPONENTS

The main component of a PV system is the PV module; whose models we have already approached in the last section. Other components are the MPPT (Maximum Power Point Tracker) and the inverter, which we will approach in this section.

4.1 MPPT – MAXIMUM POWER POINT TRACKER

As seen before, the PV module DC output power changes with atmospheric conditions (irradiance and temperature) and with the terminal voltage. Let us look back at Figure 3-4, where an I-V curve is depicted. In general, any point of the I-V curve is a valid operating point, but only one is desired – the one that corresponds to the maximum DC output power, for the given conditions of irradiance and temperature. In Figure 3-4, this point is highlighted as P_p, because that I-V curve refers to STC.

The maximum output power occurs for a particular voltage, the so-called maximum power voltage, V_{MP}. In the MPPT, this voltage is computed through a dedicated algorithm. The voltage reference value as calculated by the MPPT is the input of a DC/DC converter that adjusts the output voltage to the input voltage of the inverter.

In this way, it is assured that the PV module always operates in optimal conditions, because the maximum possible output power for the given conditions of irradiance and temperature is achieved. This highlights the need for accurate and efficient maximum power computation through appropriate simulation models, because PV modules are expected to operate always at maximum power point, for the existing irradiance and temperature conditions.

Most inverters on the market today perform (MPPT) function, meaning that the MPPT is incorporated inside the inverter, however current trends point to a separate MPPT.

4.2 INVERTER

PV systems convert solar radiation energy into electricity. The physical phenomena related to this conversion imply that the output of a PV system is Direct Current (DC). Most of the PV systems in operation worldwide are connected to the power system, which is operated in Alternate Current (AC). Therefore, the PV system DC output power must be converted into an AC power, with proper voltage and current characteristics (both in terms of magnitude and frequency) suitable to be injected into the grid. In order to perform this conversion, an interface device, the inverter, is required. The inverter is an electrical equipment, composed by power electronics devices, whose objective is to convert DC electrical quantities into AC electrical quantities. For this reason, the inverter is also known as DC/AC converter.

Nowadays, the inverters used in PV systems are very complete, namely including in the same device the functions of:

- DC/AC conversion (inverter function) with high quality standards.
- Maximum power tracking (MPPT function), i.e., regulating the voltage to the value corresponding to the maximum power. In modern PV systems, this function tends to be performed by a separated DC/DC converter.
- System protection, namely, overload, overvoltage, frequency, interconnection, detection of island, etc. Islanding occurs whenever the grid is disconnected and PV systems keep feeding isolated consumers. This operating mode is normally forbidden by the grid codes. Nevertheless, it is technically possible, providing that PV systems are adequately designed for that purpose.

4.2.1 Inverter configuration

Inverters for PV systems can be classified accordingly to their position on the terrain, as follows:

- Central inverter (Figure 4-1a)
- String inverter (Figure 4-1b)
- Multi-string inverter (Figure 4-1c)
- Module integrated inverter (Figure 4-1d)

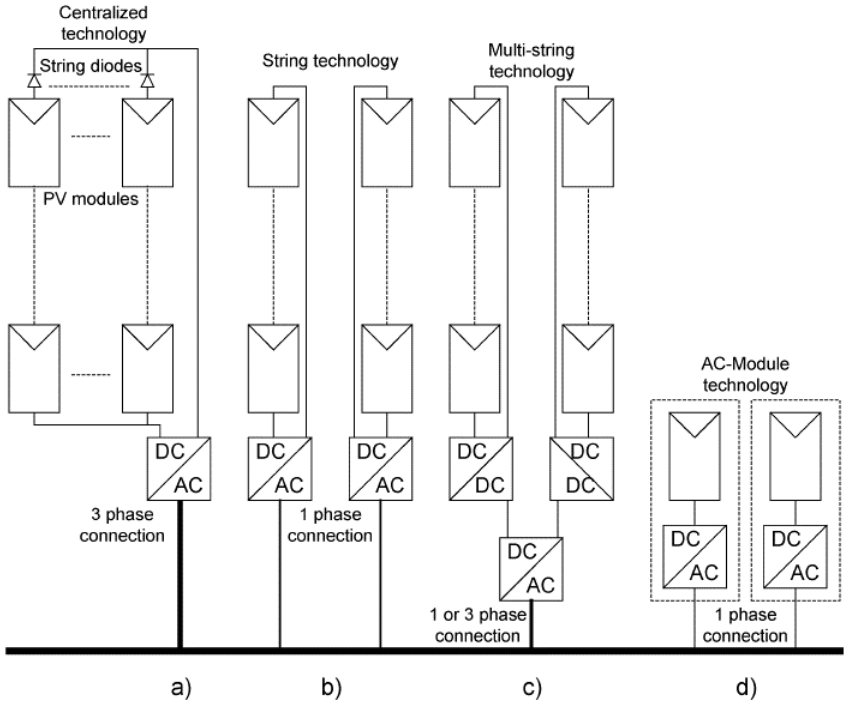

Figure 4-1: Types of grid connected inverters for PV systems: (a) central inverter; (b) string inverter; (c) multi-string inverter; (d) module integrated inverter.

Central inverter – This was the configuration used in the first grid connected PV parks: the series and parallel connected modules are coupled to a single central inverter, which integrates both the MPPT and DC/AC inverter functions. Each series connected module string has a diode to prevent current flow circulation between strings (string diode in Figure 4-1a). The increase in the voltage as obtained by the series connection is enough to fulfil the input voltage requirements of the inverter. This type of configuration presents some disadvantages: (i) increased losses, due to the centralized location of the inverter (local control of each module

optimal voltage is impossible, only module ensemble control is performed); (ii) need for High Voltage (HV) DC cables to allow for the connection of the PV modules to the central inverter; (iii) design with little flexibility; (iv) relatively high price. Mass production was not reached, mainly due to these drawbacks.

String inverter – Nowadays, this is the most used configuration to connect big PV parks to the grid. Each string of series connected PV modules is coupled to its own inverter, therefore there is no need for string diodes (Figure 4-1b). Nominal capacity of each inverter is *1/n* of the nominal capacity of the equivalent central inverter, being *n* the number of strings. In general, the string voltage is enough to feed the inverter, as so, no voltage amplification is necessary. If that is not the case, a DC/DC boost converter is required. String inverter configuration show some advantages: (i) each string has its own MPPT, thus losses are reduced; (ii) reduced costs, due to mass production; (iii) improved overall efficiency.

Multi-string inverter – Each string is coupled to a common DC/DC converter (including the MPPT), which, in turn, feeds a unique inverter with a simplified control system (Figure 4-1c). The advantages of the configurations "string inverter" and "module integrated inverter" are combined in this configuration, also known as Smart PV Panel. Each PV module string is individually controlled, therefore increasing the overall efficiency. Moreover, costs are reduced and the design has improved flexibility. This technology is currently showing major developments.

Module integrated inverter – This option represents the integration of both the inverter and the PV module into a unique electrical device (Figure 4-1d), known as AC module. The inverter is mounted inside or below the PV module, thus temperature related constraints must be taken into account. Module integrated inverters, or micro-inverters, are used in low power applications, typically in the range 200-300 W. They present both MPPT and inverter functions, therefore it is assured that each module operates always at maximum possible power point. This feature is especially important, because AC modules are normally used in

urban environments where shading effects may occur. Other advantages may be outlined: increased modularity, easy plug-and-play installation and improved security. The disadvantages of this approach are mainly related to the high per unit power cost, the central inverter being the best solution as far as this parameter is concerned. Nevertheless, this drawback may be overcome if AC modules tends to become the generalized solution.

4.2.2 Inverter types

Inverters can be classified accordingly to the way semiconductor commutation is performed, as can be seen in Figure 4-2.

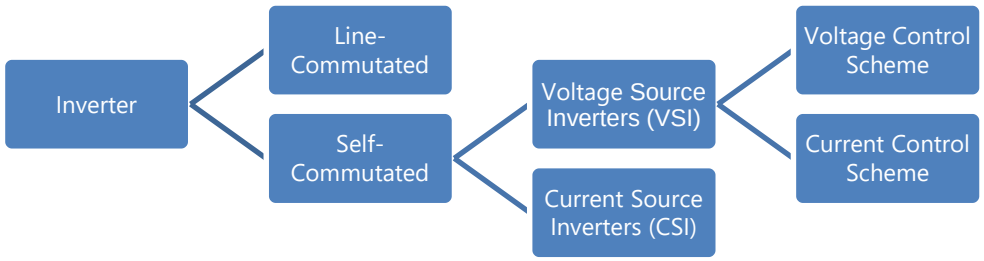

Figure 4-2: Inverter types.

Line-commutated inverters use the thyristor as the commutation element. Thyristors are semi commanded devices, because they allow for ON-state control, but they are unable to control the time instant in which they go to OFF-state. OFF-state is achieved when current is zero, therefore either grid AC voltage support is needed or auxiliary circuitry with the same objective. Its operating principle implies rectangular waveforms to be obtained, with a high harmonic content. High harmonic content and the associated reactive power needs are one of the reasons why modern inverters are no longer equipped with thyristors.

Modern inverters are totally commanded, i.e. self-commutated, both ON-state and OFF-state being controlled. IGBT (Insulated Gate Bipolar Transistor) and

MOSFET (Metal Oxide Semiconductor Field Effect Transistor) are the used semiconductor devices, the former being more used than the latter. These devices are able to operate at high switching frequencies, let us say, tens or even hundreds of kHz. They allow for accurate control of voltage and current on the AC side, adjusting power factor and reducing the harmonic content. This type of inverters is currently being widely used in PV systems. Possible electromagnetic compatibility issues, due to high switching frequencies, are to be monitored.

Self-commutated inverters can be Voltage Source Inverters (VSI) or Current Source Inverters (CSI). The main difference between these two types of inverters is related to the DC side representation: VSI represent the DC side as a voltage source whereas CSI represent it as current source. Both of them allow for a constant magnitude and variable frequency waveform to be obtained in the AC side. In PV systems VSI are normally used because the output quantity of a PV module is a DC voltage. When seen from the AC side, VSI can be operated as a voltage source or as a current source depending on the used control system.

In the voltage control scheme, the target voltage is given as a reference and the objective of the control system is to obtain that very same voltage waveform. Pulse Width Modulation (PWM) technique is normally used: commutation time interval is determined by the comparison between the target sinusoidal waveform and a high frequency triangular waveform, leading to a constant magnitude and variable width impulse control signals to be obtained. This type of inverters can be used in off-grid applications.

On the other hand, the target current waveform is given as a reference in the current control scheme and the output voltage is controlled till the target current waveform is obtained.

VSI with current control scheme are normally used in grid-connected PV systems. Effective power factor control using relatively simple control circuits and the pos-

sibility of controlling the current when the grid is disturbed are the main advantages of this configuration. This type of inverters cannot be used in off-grid applications.

Grid connection through inverters should not spoil power supply quality. Modern inverters harmonic content, which is measured by the THD (Total Harmonic Distortion), is usually less than 3%. In many cases, this is a figure that is better than the figure corresponding to the public grid power supply, because nowadays there is a significant number of electronic devices connected to the grid that damage power quality.

4.2.3 Inverter efficiency

An important aspect is the overall efficiency of the interface device between the PV modules and the grid. The efficiency of the inverter is given by:

$$\eta_{inv} = \frac{P_{AC}}{P_{DC}} \qquad \text{equation 4.1}$$

In equation 4.1, P_{AC} and P_{DC} are the active powers in the AC and DC sides, respectively.

Inverters are high performance devices in the DC/AC conversion. Peak efficiency is usually between 85% and 96% for power values close to the rated power. When the output power is considerably lower than the rated power, for instance, in cloudy sky conditions, in the start-up, or at sunset or sunrise, the efficiency significantly drops.

Typical inverter efficiencies as a function of the AC output power in percentage of the rated power can be seen in Figure 4-3.

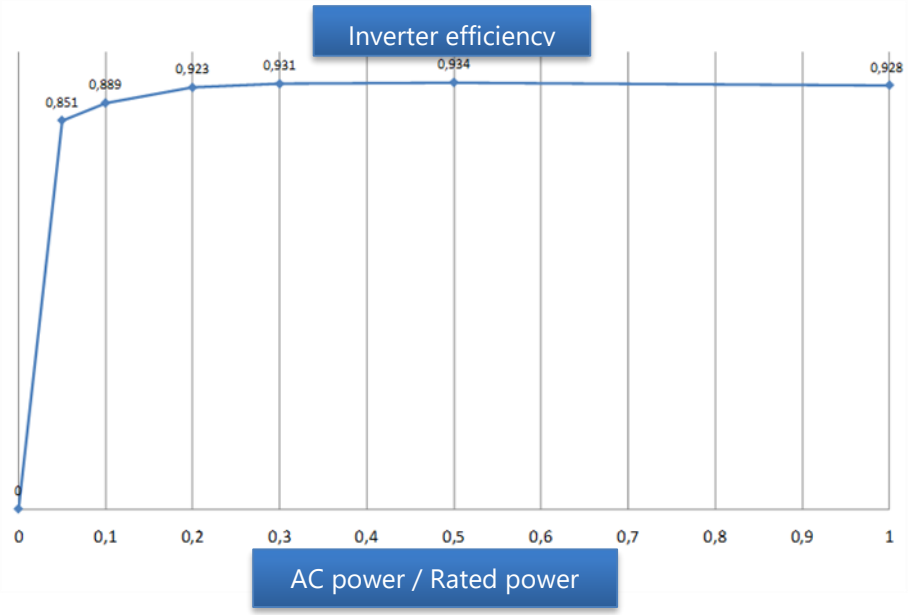

Figure 4-3: Typical efficiency curve of grid-connected PV inverters.

The simpler inverter models, known as efficiency models, consider that the inverter losses can be approximated by a quadratic expression that depends on the input DC power, as shown in equation 4.2.

$$\eta_{inv} = \frac{P_{AC}}{P_{DC}} = \frac{P_{DC} - \left(a + bP_{DC} + cP_{DC}^{2}\right)}{P_{DC}} \qquad \text{equation 4.2}$$

We remark that equation 4.2 is written in terms of the input DC power, because this is the quantity that comes out from PV performance models. This formulation includes: a constant parcel to model self-consumption; a linear parcel to describe the voltage drop along the semiconductors; and a quadratic parcel to account for Joule losses.

For the typical inverter whose efficiency is depicted in Figure 4-3, numerical values for equation 4.2, considering that P_{DC} is in pu (base power = inverter rated power), are as follows:

$$\begin{aligned} a &= 6.0878 \times 10^{-3} \\ b &= 0.0473 \\ c &= 0.0164 \end{aligned} \qquad \text{equation 4.3}$$

When the performance of several inverters is to be compared, a uniform metrics is convenient. As a consequence, the European Efficiency has been defined as a weighted average of the inverter efficiency at different load operating points:

$$\eta_E = 0.03\,\eta_{5\%} + 0.06\,\eta_{10\%} + 0.13\,\eta_{20\%} + 0.10\,\eta_{30\%} + 0.48\,\eta_{50\%} + 0.20\,\eta_{100\%}$$ equation 4.4

In equation 4.4, η_E is the European Efficiency and $\eta_{i\%}$ is the inverter efficiency at i% of the rated power.

The European Efficiency of the typical inverter whose efficiency curve is shown in Figure 4-3 is 0.9259.

5 ELECTRICITY DELIVERED TO THE GRID

The objective of this chapter is to provide a methodology to compute the electricity that is injected in the grid by a PV module.

We have seen that the DC power output of a PV module depends upon the irradiance and module temperature. Therefore, we assume that information about these two quantities must be available, through dedicated measurements.

5.1 INPUT DATA

Let us begin by the irradiance information, which can be measured using a device called a pyranometer. But before that let us take a look at the sun irradiation received on a tilted plane. Figure 5-1 shows the monthly sun irradiation received in each square meter of terrain in Lisbon for different tilted planes. It is apparent that the 30º slope is the one that maximizes the sun irradiation over one year. Therefore, this is the recommended tilt for PV modules installed in the Lisbon zone.

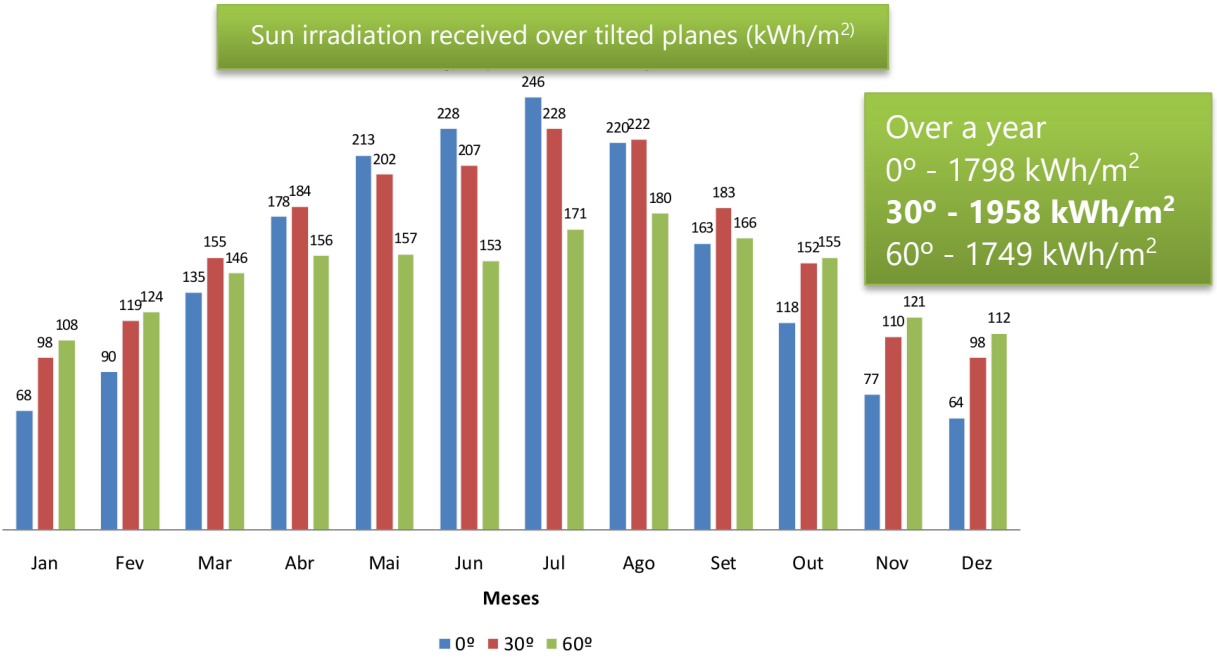

Figure 5-1: Monthly sun irradiation received over tilted planes in Lisbon.

Figure 5-2 portrays the monthly irradiance over a 30º tilted plane in Lisbon. Each bar is the monthly average computed based on hourly averages.

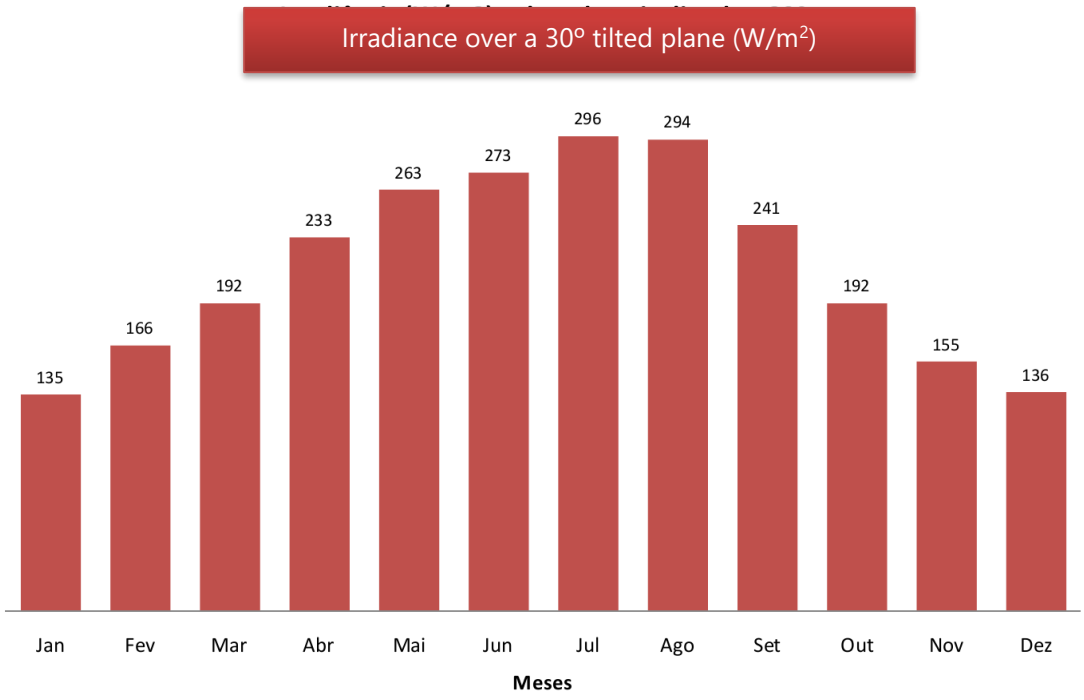

Figure 5-2: Monthly average irradiance in Lisbon over a 30º tilted plane.

Figure 5-3 shows the respective histogram based on hourly average measurements and in 100 W/m^2 intervals. One can conclude that each bin occurs more or less with the same frequency.

Irradiance information can be provided on a different time scale. For instance, Figure 5-4 shows an example of the irradiance over the period of one week with a sampling rate of one minute for the winter and for the summer. In this figure, besides global irradiance, diffuse irradiance is also shown. It is apparent that cloudy days make the variation pattern very spiky, deviating from the known bell-shaped pattern of clear sky days. Of course, this has an impact on the PV output power. As expected, peak irradiance is higher in summer than in winter.

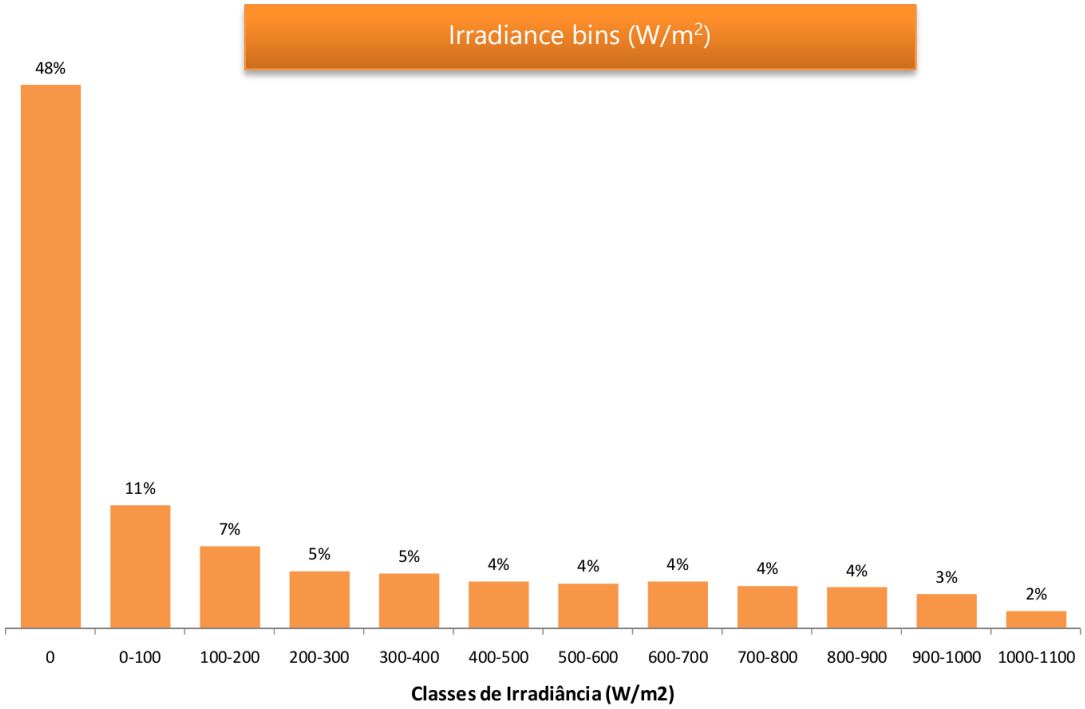

Figure 5-3: Irradiance histogram in Lisbon.

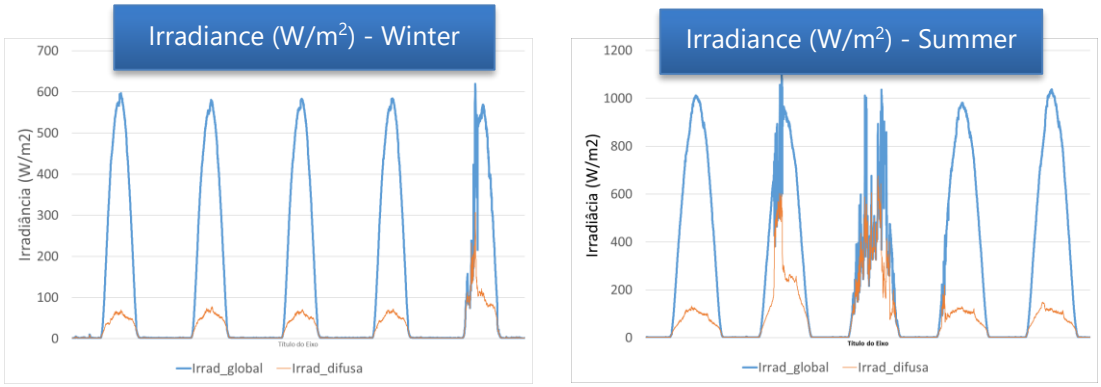

Figure 5-4: Example of irradiance over a winter (left) and summer (right) week; blue – global irradiance; orange – diffuse irradiance.

The other input that it is required to be known as an input of the model is the module temperature. However, this data will be only available after the installation of the system, not before. Before the installation of the physical system, the quantity that is available through measurements is the ambient temperature. Figure 5-5 shows the monthly average ambient temperature in Lisbon.

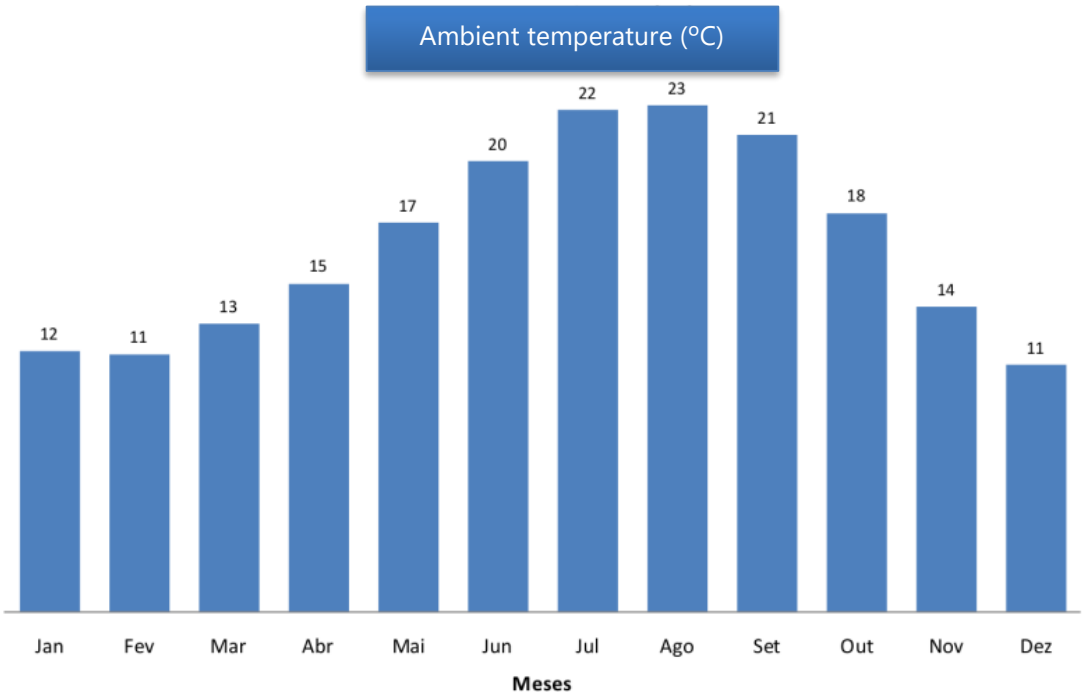

Figure 5-5: Monthly ambient temperature in Lisbon.

We should now devise a way of estimating the module temperature, the one that really interests, from the ambient temperature. To do that, we are going to introduce a simple model (known as Ross model) that assumes that the module temperature is linearly dependent on the irradiance, that is:

$$\theta_m = \theta_a + kG \qquad \text{equation 5.1}$$

where θ_m is the module temperature, θ_a is the ambient temperature and G is the irradiance.

The k constant can be determined if an operating point is known. Datasheet information provides a quantity called NOCT, which stands for Normal Operating Conditions Temperature. As seen in Table 3-1, this is the module temperature under Normal Operation Conditions (NOC), internationally defined as G^{NOC} = 800 W/m^2 and $\theta_a^{NOC} = 20\ ^\circ C$. Replacing these known operating point in equation 5.1, one obtains:

$$NOCT = 20 + 800\,k \qquad \text{equation 5.2}$$

and therefore, the general equation that allows the computation of the module temperature from the ambient temperature and irradiance is:

$$\theta_m = \theta_a + \frac{NOCT - 20}{800} G \qquad \text{equation 5.3}$$

A typical value for NOCT is 45 ºC. Considering this value, the module temperature, given the irradiance presented in Figure 5-2, and ambient temperature presented in Figure 5-5, is shown in Figure 5-6.

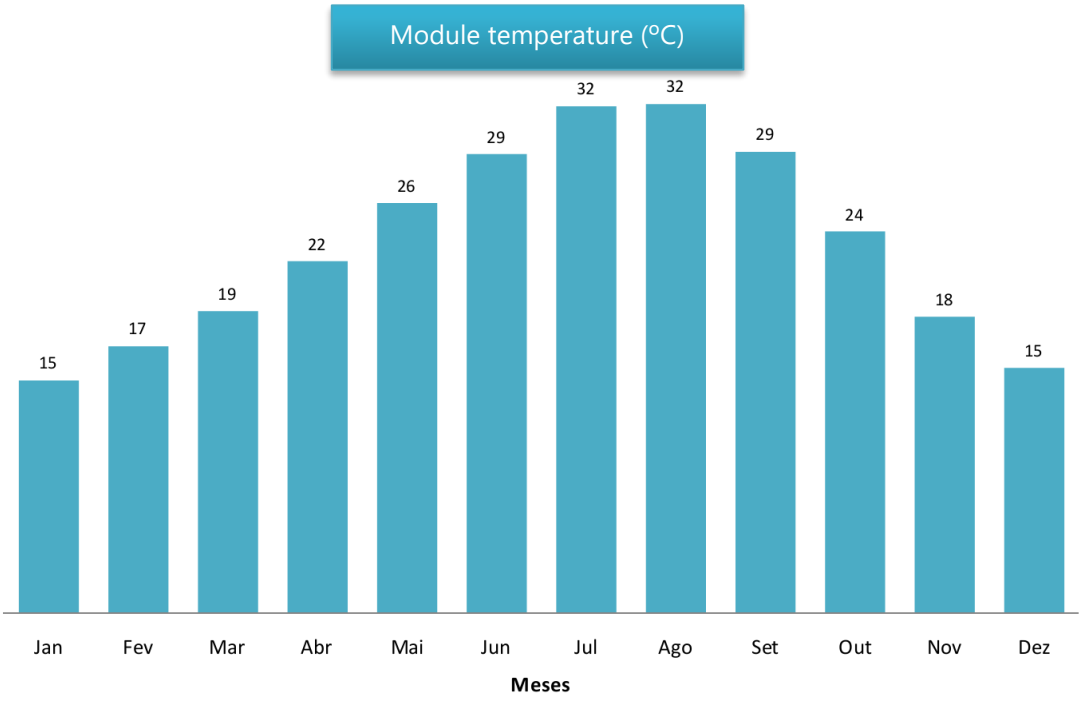

Figure 5-6: Monthly module temperature in Lisbon.

We should highlight that this is a simplified model, whose results are estimations. In Figure 5-7 we show a comparison of the measured module temperature (in blue) and the module temperature as foreseen by Ross model (in orange), for one winter day (left) and for a summer day (right).

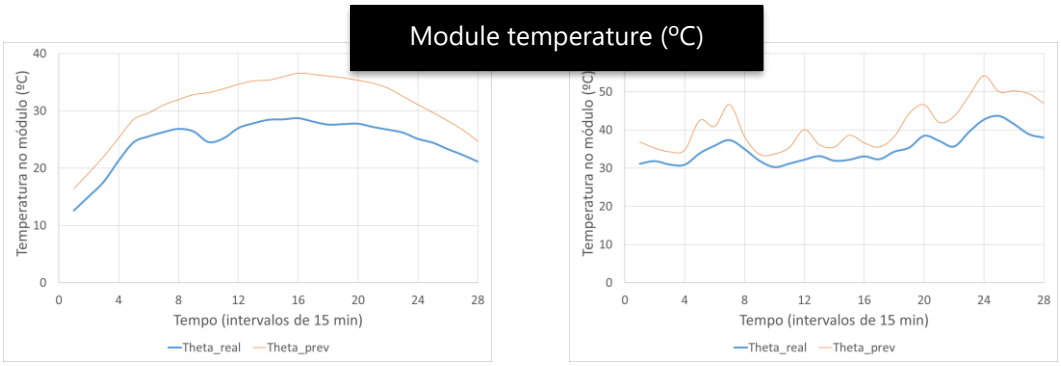

Figure 5-7: Comparison of measured module temperature (blue) with module temperature as foreseen by Ross model (orange) for a winter day (left) and for a summer day (right).

5.2 Output Annual Electrical Energy

The output annual electrical energy is given by:

$$E_a = \sum_{i=1}^{n} \eta_{inv}(P_{DC})_i P_{DC}(G,T)_i \Delta t_i \qquad \text{equation 5.4}$$

In equation 5.4, the quantities are as follows:

- E_a – Total PV electricity injected in the grid.
- η_{inv} – Efficiency of the power electronics, namely the inverter; in general, it depends on the DC output power level.
- n – Total number of time intervals.
- P_{DC} – Depending on the desired accuracy, it can be computed using: 1D+3P model (in general, more accurate); 1D+3P model with the simplified computation of PDC (intermediate accuracy); Fast Estimate (in general, less accurate).
- Δt – Time interval.

6 OTHER SUN POWER – CONCENTRATING SOLAR POWER

Power available in sun radiation can be used in other ways, rather than in PV systems. A completely different way of using sun power is CSP – Concentrating Solar Power. The operating principle is similar to the conventional thermal power plants: water is overheated in a boiler; steam is produced and is expanded in a steam turbine; electricity is produced via a generator.

The difference is in how steam is produced. In thermal power plants, steam is produced from the combustion of a fossil fuel (coal, natural gas…). In CSP installations, sunlight is focused on a receiver to obtain high temperature heat and produce steam. To focus the sunlight, mirrors or lenses equipped with solar position tracking systems are used.

Figure 6-1 shows a diagram of a CSP plant.

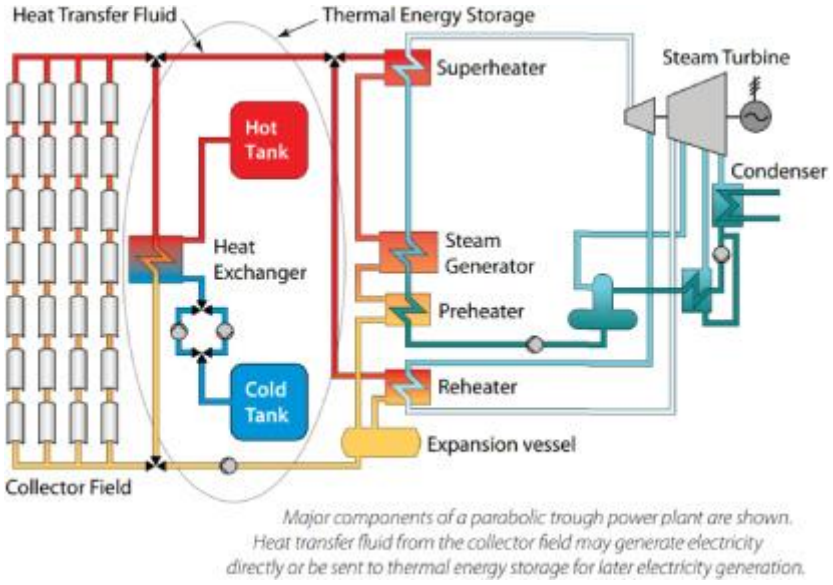

Figure 6-1: Diagram of a CSP plant; Source: https://epress.lib.uts.edu.au/student-journals/index.php/PAMR/article/view/1392/1471

Many CSP installations have thermal energy storage, therefore allowing the plant to operate even without sunlight. Usually, a huge metal tank stores the hot liquid, whether in molten salts or in a heat transfer fluid.

Spain (2300 MW, in 2016) and the USA (1700 MW, in 2016) are the countries with more CSP installed. Nevertheless, the costs are still higher than PV, what is hindering its development.

There are several different technologies that use CSP concept. The ones that are currently more mature are parabolic troughs and solar tower.

6.1 PARABOLIC TROUGHS

In this CSP technology, sunlight is concentrated using big rectangular mirrors curved in a parabolic shape, each with long heat collector pipes, as shown in Figure 6-2.

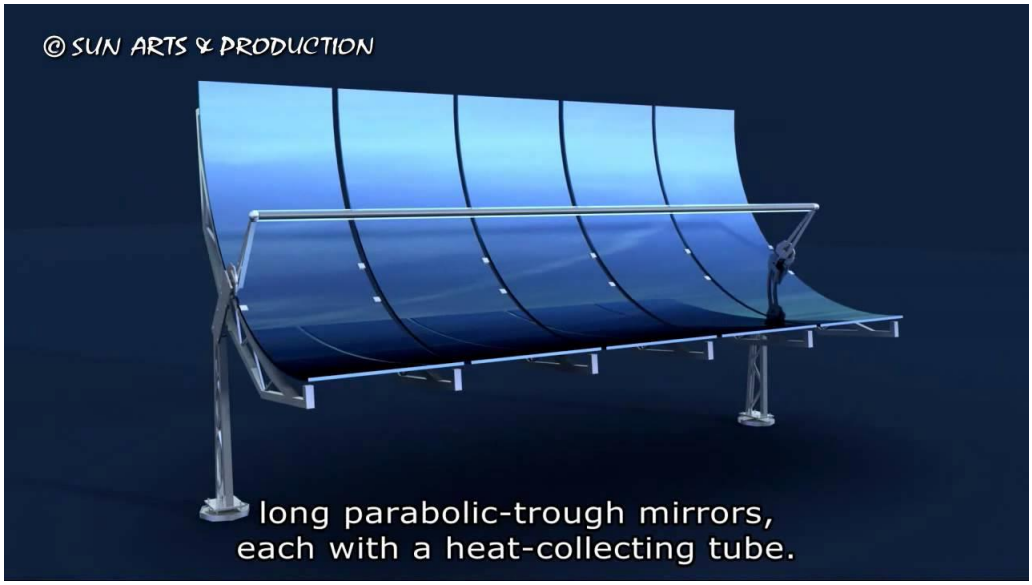

Figure 6-2: Parabolic trough.

The system features a 1 axis sun tracking system and the concentration ratio achieves values between 70 and 100. Inside the pipes, there is a heat transfer fluid, which is heated to a high temperature (around 400ºC), capable of generating steam into a heat exchanger. As heat transfer fluid, current plants use some synthetic oil, but alternative concepts include direct steam generation, and the use of molten salts as transfer fluid.

Troughs represent the most mature technology and the bulk of current projects; some have significant storage capacities. The solar to electricity conversion can reach an efficiency between 10% and 15% (annual mean value).

Figure 6-3 shows a picture of a parabolic trough power plant.

Figure 6-3: Parabolic trough power plant; Source: https://www.sbp.de/en/project/parabolic-trough-power-plant-andasol-ii/.

6.2 Solar Tower

Solar tower is another CSP technology. It uses a field of distributed flat, sun-tracking mirrors – heliostats – that individually track the sun and focus the sunlight on the top of a tower. A picture of the heliostats field is shown in Figure 6-4. We highlight that these are mirrors, not PV arrays.

By concentrating the sunlight 600–1000 times, they can achieve temperatures from 600–800°C. A heat-transfer fluid heated in the receiver is used to heat a working fluid, normally molten salt. A cold tank and a hot tank store the working fluid. In a heat exchanger the solar energy absorbed by the working fluid is used to generate steam to power a conventional turbine. The average efficiency is in the range of 10%. Figure 6-5 shows a picture of a solar tower power plant.

Figure 6-4: Heliostats filed in a solar tower power plant; Source: https://www.alamy.com/stock-photo-juelich-germany-solar-power-tower-juelich-54540599.html.

Figure 6-5: Solar tower power plant; Source: https://inhabitat.com/the-las-vegas-strip-could-soon-be-powered-by-a-solar-tower/.